Organic Fouling on Zwitterionic Amphiphilic Copolymers: Implications in Biofouling

Journal:	*ACS Applied Materials & Interfaces*
Manuscript ID	Draft
Manuscript Type:	Article
Date Submitted by the Author:	n/a
Complete List of Authors:	Wang, Meng; University of Houston, Civil and Environmental Engineering Sarma, Murchana; University of South Carolina, Environmental Engineering and Earth Sciences Lounder, Samuel; Tufts University, Chemical and Biological Engineering Mondal, Abhishek; Vanderbilt University, Chemical and Biomolecular Engineering Muthusamy, Lavanya; Clemson University Koley, Goutam; University of South Carolina, Electrical Engineering Asatekin, Ayse; Tufts University, Chemical and Biological Engineering Rodrigues, Debora; University of Houston, Civil and Environmental Engineering

Organic Fouling on Zwitterionic Amphiphilic Copolymers: Implications in Biofouling

Meng Wang[1$], Murchana Sarma[3$], Samuel J. Lounder[2], Abhishek N. Mondal[2], Lavanya Muthusamy[4], Goutam Koley[4], Ayse Asatekin[4], Debora F. Rodrigues[3*]

[1]Department of Civil & Environmental Engineering, University of Houston, Houston, TX 77004, United States

[2]Department of Chemical and Biological Engineering, Tufts University, Medford, Massachusetts 02155, United States

[3]Department of Environmental Engineering and Earth Sciences, Clemson University, Clemson, South Carolina, 29634, United States

[4]Holcombe Department of Electrical and Computer Engineering, Clemson University, Clemson, South Carolina 29634, United States

$: Equal contribution.

*Corresponding authors: dfrodri@clemson.edu

Phone: 864-656-3519

Abstract

Zwitterionic Amphiphilic Copolymers (ZACs) have shown promise in resisting attachment of oil emulsions, proteins, and organic biomolecules, suggesting their potential to prevent microbial adhesion as well. However, there is a lack of comprehensive studies exploring the role of ZACs in regulating cell deposition and subsequent biofilm formation on surfaces. Here, we fabricated ZAC coatings including poly-(trifluoroethyl methacrylate-random-sulfobetaine methacrylate) (PTFEMA-*r*-SBMA or PT:SBMA), poly(trifluoroethyl methacrylate-random-2-methacryloyloxyethyl phosphorylcholine) (PTFEMA-*r*-MPC or PT:MPC), poly(methyl methacrylate-random-sulfobetaine methacrylate) (PMMA-*r*-SBMA or PM:SBMA), and poly(methyl methacrylate-random-2-methacryloyloxyethyl phosphorylcholine) (PMMA-*r*-MPC or PM:MPC). These coatings were assessed for their resistance to conditioning with organic molecules, attachment of Gram-positive, *Bacillus subtilis* TR11 (*B. subtilis*), and Gram-negative, *Escherichia coli* K12 (*E. coli*), bacteria, and subsequent biofilm formation. Surface characterizations highlighted the role of organic molecule conditioning from the media in altering the ZAC-coated surface properties, subsequently influencing bacterial deposition and biofilm growth. Cell deposition results revealed that all ZAC coatings displayed higher resistance to *B. subtilis* attachment compared to *E. coli*, indicating that bacterial adhesion to the surfaces depends on the type of bacteria. Among the tested ZAC coatings, PT: SBMA demonstrated the highest potential for resisting adhesion by both types of bacterial cells, as well as exhibiting lower surface energy, and lower roughness after organic medium conditioning. These findings contribute to enhancing our fundamental understanding of how zwitterionic materials control biofouling.

Keywords: zwitterionic amphiphilic copolymers (ZACs), coatings, *Bacillus subtilis* TR11, *Escherichia coli* K 12, Biofouling.

1. Introduction

Bacterial cells are ubiquitous in nature, existing either as freely suspended planktonic cells or as biofilms that attach to surfaces.[1–6] Biofilm formation presents substantial challenges across multiple industries, including membrane treatment processes,[7–9] marine environments,[6,10] and medical devices.[5,11] Microbial biofilms are complex, three-dimensional communities of microorganisms that adhere to surfaces. Biofilm growth is initiated through the conditioning of surfaces with organic molecules from the growth medium or the environment, followed by the initial attachment of bacteria to the surface, and subsequent growth and proliferation of cells at the interfaces.[12,13]

To curtail the formation of biofilm on surfaces, many researchers have proposed that hydrophilic and neutrally charged surfaces could be used. Therefore, hydrophilic polymers such as zwitterionic polymers, poly (ethylene glycol) (PEG),[14] poly (acrylamides),[15] and poly(acrylates)[16] have been used to coat surfaces. These polymers have also been shown to present antifouling performance. While the latter three polymers corroborated the hydration-induced antifouling principle via hydrogen bonding,[15] such interactions between polymers and water molecules are relatively easy to break, which could impact their antifouling performance.[17] On the other hand, the unique structures of zwitterionic materials have been suggested to make ideal candidates for producing anti-fouling surfaces.[18,19]

Zwitterionic (ZI) polymers have a unique structure with equal numbers of cationic and anionic groups, resulting in charge neutrality and high hydrophilicity.[20] Such characteristics have been proposed to make them highly suitable for combatting persistent fouling issues by effectively preventing the attachment of organic molecules, such as proteins to surfaces.[15,16,21] The fouling

prevention mechanisms of ZI polymers were attributed to the excellent hydration capabilities of the material via strong electrostatically driven hydration.[22] Comparisons with unmodified membranes and ZI-coated membrane surfaces revealed better performance of the modified membranes by reducing membrane flux decay caused by foulant adsorption. These results suggest the potential of ZI polymers for membrane modifications.[15,17,23] Furthermore, zwitterionic monomers can be copolymerized with various hydrophobic monomers to create copolymers known as Zwitterionic Amphiphilic Copolymers (ZACs), which can resist the fouling caused by different organic molecules including proteins, alginate, dyes, and oil emulsions.[24–31] ZAC-based membranes exhibit some of the highest levels of organic fouling resistance in the literature, enabling the filtration of wastewaters with extremely high oil and organics content. Interestingly, even highly hydrophobic ZAC surfaces can offer significant resistance to protein adsorption, indicating more complex mechanisms of adsorption prevention.[27] Though ZACs have been extensively studied for organic fouling resistance in the context of filtration membranes, research on their effectiveness in mitigating bio-fouling remains an unexplored research gap. Unlike organic fouling, which involves non-living materials like proteins and lipids, bio-fouling involves living organisms such as microorganisms and algae that grow and interact dynamically with surfaces, often influenced by organic matter.[2,32,33] Thus, understanding the role of organic conditioning in bio-fouling is essential.

This study aimed to investigate the interactions between different types of ZACs and various bacterial strains concerning biofilm formation. Four copolymers containing different combinations of hydrophobic monomers (2, 2, 2-trifluoroethyl methacrylate (TFEMA) or methyl methacrylate (MMA)) and hydrophilic zwitterionic monomers (sulfobetaine methacrylate (SBMA) or methacryloxyphosphorylcholine (MPC)) were synthesized, and their resistance to biofouling was

assessed with two commonly studied microorganisms, the Gram-positive *B. subtilis,* and the Gram-negative *E. coli*. In the experiments, the initial cell deposition kinetics, and the subsequent formation of biofilm on different ZAC coatings were quantified and compared. To shed light on the underlying mechanisms governing the behavior of microorganisms on different ZAC coatings, comprehensive surface characterizations were conducted both before and after conditioning the coated surfaces with the growth medium, which is rich in diverse organic molecules.

2. Materials and Methods

2.1 Synthesis of zwitterionic copolymers

According to the protocols that were described in our previous publications, [34] the free-radical polymerization (FRP) method was used to synthesize four different types of zwitterionic amphiphilic copolymers (ZACs), combining one of two hydrophobic monomers, 2, 2, 2-trifluoroethyl methacrylate (TFEMA, abbreviated in copolymer structures as PT), methyl methacrylate (MMA, abbreviated in copolymer structures as PM), with one of two zwitterionic monomers, sulfobetaine methacrylate (SBMA) or methacryloxyphosphorylcholine (MPC). Briefly, the monomers were dissolved in dimethyl sulfoxide (DMSO) or ethanol, depending on the specific combination of monomers, with the addition of lithium chloride (LiCl) to improve solubility. The free radical initiator azobisisobutyronitrile (AIBN) was added, and the mixture was purged with nitrogen gas for 20 minutes to remove dissolved oxygen. The reaction was conducted in a sealed round-bottom flask at 70°C for 20 hours in a heated oil bath under stirring. After polymerization, the copolymers were precipitated by transferring the reaction solution into a non-solvent mixture (e.g., ethanol/hexane (*v:v=1:1*) or tetrahydrofuran (THF)). The precipitated polymers were then cut into small pieces, washed thoroughly multiple times with ethanol or isopropanol, air-dried, and

further dried in a vacuum oven at 50°C for 20 hours. The final copolymer composition was characterized by ^{1}H-NMR using DMSO-d6 with a small amount of LiCl as the solvent, using a delay time of 10 s. Detailed synthesis procedures are provided in **Text S1** of the Supporting Information. Additional details, including chemical structures and ^{1}H NMR spectra of all ZACs used in this study, have been reported in our prior work.[34] The four ZACs used in this study were poly(trifluoroethyl methacrylate-*r*-sulfobetaine methacrylate) (PT:SBMA, 36 *wt.*% SBMA), poly(trifluoroethyl methacrylate)-*r*-methacryloxyphosphorylcholine (PT:MPC, 34 *wt.*% MPC), poly(methyl methacrylate)-*r*-sulfobetaine methacrylate (PM:SBMA, 40 *wt.*% SBMA), and poly(methyl methacrylate)-*r*-methacryloxyphosphorylcholine (PM:MPC, 34 *wt.*% MPC).[25,26,34,35]

2.2 Preparation of copolymer film

To prepare ZAC coatings, glass slides were selected as substrates. Before the coating, the slides were cleaned with acetone, isopropyl alcohol, and ethanol sequentially to remove any other bio-contaminants. These selected ZACs were first dissolved in 2, 2, 2-trifluoroethanol (TFE) at 50 °C to make a 3 *wt.* % solution. The copolymer solutions were filtered using a 0.45 μm syringe filter made of polytetrafluoroethylene (PTFE, Wheaton Co.) and degassed by heating to 50 °C in a sealed vial for 1 h until no visible gas bubbles were observed.[34] After that, a 120 μL solution was spin-coated on the glass slides. The samples were spun at 500 rpm for 20 s, and then 2000 rpm for 1 min. It should be noted that, prior to spin coating, the glass substrates were treated with UV/ozone for 10 minutes to enhance the adhesion of the zwitterionic amphiphilic copolymers onto their surfaces. The successful coating was determined using Attenuated Total Reflection Fourier-transform Infrared Spectroscopy (ATR-FTIR, Digital lab FTS- 700) to obtain the IR spectrum of the glass slides before and after spin coating.[34]

2.3 Characterization of copolymer coatings before and after organic conditioning

To assess the impact of organic matter in the growth medium on the surface properties of ZAC coatings, glass surfaces and freshly prepared ZAC substrates were immersed in Tryptic Soy Broth (TSB) solutions for 72 hours. TSB is rich in nutrients such as peptides, salts, phosphates, and glucose and supports bacterial growth and biofilm formation. To differentiate the effects of the adsorption of the organic compounds in TSB versus the effects of swelling and polymer- salt interactions on the surface properties of ZAC coatings, an organic-free salt solution composed of 5 g/L sodium chloride (NaCl) and 2.5 g/L dipotassium phosphate was also used to treat ZAC coatings for 72 hours for further comparison. After treatment, the coatings were gently rinsed first, and then dried using Kimwipes to remove any remaining saline solution. Various characterization techniques were then employed to examine the ZAC coatings before and after conditioning with the salt and TSB solution.

To investigate the effects of the adsorption of any organic matter from the growth medium on the surface hydrophilicity of ZAC coatings, air contact angle was measured using the captive air bubble method.[34] In this experiment, wet ZAC coatings before and after 72 h of TSB and salt solution treatment were fixed on a holder, and placed upside down on the top part of a rectangular chamber prefilled with DI water.[34] An air bubble of 5 μL was dispensed on the ZAC coating surfaces from below using a syringe with a bent U-shaped needle tip. The air-in-water contact angle was captured using a Data-physics OCA 15EC goniometer with a live camera. Five triplicate measurements at different spots on the substrates were taken, and the average contact angles and their standard deviations were reported.

Tapping mode atomic force microscopy (Innova AFM - Bruker) was performed to obtain the surface roughness of ZAC coatings before and after 72 h of TSB and salt solution treatment. The

coated slides were placed on a carbon disk before the measurement, and an area of 10 μm by 10 μm was scanned for each sample at a scanning rate of 0.5 Hz. Triplicate measurements for each coating were taken, and the surface roughness was calculated based on the collected height images using the Nano-scope Analysis program, version 1.5.[36] In addition, ATR-FTIR measurements were performed to confirm the adsorption of organic matter on ZAC coatings. IR spectra of TSB, and ZACs before and after TSB solution conditioning for 72 hours were obtained in an absorbance mode within the range of 650−4000 cm^{-1}. A total of 96 scans at a resolution of 4 cm^{-1} were taken during the measurement.[37]

To investigate the effect of TSB solution on the surface charge of ZAC coatings, we employed dynamic light scattering (DLS) using a Zetasizer Nano instrument (Malvern Instruments Ltd.). The method for characterizing the surface zeta potential of both bare and ZAC-coated glass was based on detailed protocols outlined in the instrument manual[38] and previous publications.[36,37] Initially, the substrates were fixed between two electrodes and fully immersed in 1 mL of diluted TSB solution, which contains solutes such as peptides, salts, glucose, and others. Instead of the conventional tracer solution containing polystyrene latex particles, the diluted TSB solution was used to better reflect real environmental conditions.[37] However, due to the high ionic strength and complexity of the full-strength TSB medium, it was necessary to dilute the original concentrated TSB solution 100-fold in order to ensure compatibility with the instrument's operational range. The diluted TSB solution had a pH of 6.70 and a measured zeta potential of -29.42 ± 1.93 mV.

The mobility of the diluted TSB solution (used as the new 'tracer') was measured using the surface zeta potential cell kit at five distances from the substrate surface: 125, 250, 500, 750, and 3000 μm. To adjust the measurement distance, the cap on the dip cell was turned counterclockwise in 1/4-turn increments, with each increment corresponding to a displacement of 125 μm. This

approach allowed precise control over the distance between the solutes in TSB and the substrate surface, ensuring accurate mobility measurements at each location. At distances closer to the surface (125, 250, 500, and 750 μm), electro-osmotic flow dominated the mobility of TSB solutes, and the mobility was observed to decrease linearly with increasing distance from the substrate. The apparent mobility at these distances was plotted, and the resulting trend line was extrapolated to zero displacement to determine the intercept, which represents the electro-osmotic contribution at the surface (with a correlation coefficient, R^2, greater than 0.95). To calculate the surface zeta potential, the zeta potential of the diluted TSB solution was measured at 3000 μm from the substrate. At this distance, any influence from electro-osmotic flow was negligible, ensuring an accurate reference point. The surface zeta potential of the substrate was then determined using the following formula:

Surface zeta potential = – intercept + the zeta potential of TSB solution (at 3000 μm)

2.4 Characterization of bacterial surface properties

To perform bacterial surface characterization, we performed Microbial Adhesion To Hydrocarbons (MATH) tests and zeta potential measurements.[39] The two microorganisms studied were *Escherichia coli* K12, and *Bacillus subtilis* TR11. Initially, both bacteria were grown in Tryptic Soy Agar (TSA) medium plates at a temperature of 30 ^{0}C for 24 h. The cells were inoculated in TSB media for 24 h for the MATH test and centrifuged for 15 min at 5000 rpm. Following centrifugation, the cells underwent two rounds of washing, each with 15 mL of Phosphate Buffer Saline (PBS). After the washing steps, the cells were re-suspended in TSB media, with their concentrations adjusted to either an optical density (OD_{600}) of 1.0 or 0.5. These prepared cell suspensions were then divided into 4 mL aliquots, to which 1 mL of hydrocarbons, specifically

hexane and decane, were introduced. After this step, the cells were vigorously vortexed for 30 s. Then, the cells were allowed to rest for 30 min to facilitate phase separation. The MATH value was calculated from the change in the OD_{600} as follows:[40]

MATH (%) = (OD_{600} after treatment) ×100/(OD_{600} before treatment),

Hydrophilicity here is defined as the amount of total cells divided into the aqueous phase, and the portion of total cells segregated into the hydrocarbon phase is defined as hydrophobicity.[41]

The zeta charge of the microorganism was measured with the Zetasizer Nano-ZSP (Malvern Industry Ltd). The microorganism was grown until the late log phase, which took place in about 7-8 h after initial inoculation of the microorganisms (OD_{600}=0.6) and then centrifuged at 5000 rpm for 10 min. The cells were then re-suspended and adjusted to OD_{600}=0.6 in PBS and their growth media (TSB for *E.coli* and *B. subtilis*). The zeta potentials were measured with the suspensions at room temperature.

2.5 Cell deposition experiments

Cell deposition experiments were done to investigate the resistance of the different copolymer coatings in repelling or attracting the bacterial cells. The bacteria investigated included E. *coli* K12 and *B. subtilis* TR11. An isolated colony from a TSB plate grown overnight for each isolate was transferred to 20 mL of TSB medium, and triplicate samples were prepared from this enrichment. The samples were incubated for around 5-6 h at 30 ℃. After incubation, cells were washed three times with PBS by centrifugation at 10,000 rpm for 15 min and re-suspended in TSB media to 0.1 absorbance at OD_{600}.

For cell adhesion experiments, 2 × 2 cm glass slides were coated by each ZAC by spin coating at 500 rpm for 20 s, and then 2000 rpm for 1 min. A "well" that would hold the bacterial solution during the cell deposition experiment was created using a single-side press-to-seal silicone tape (Sigma-Aldrich). The tape was cut into a hollow circular shape with a 20 mm diameter and 1.0 mm thickness using scissors, and then adhered to the coated slide. A volume of 25 μL of the cell suspension was added to the well, which allowed the solution to remain in place while a square coverslip was placed on top to prevent drying during the experiment, as illustrated in **Figure 1**.

During the experiment, the substrates were observed under an optical microscope (Olympus BX53) at 40× magnification. The microscope was equipped with a monochrome camera (Olympus XM10 monochrome camera) to acquire images and record videos at up to 30 fps (frames per second) with images captured every 5 minutes to monitor the cell deposition rate (**Figure S7**). Briefly, in this experiment, both attached cells and suspended cells were visible under the microscope. However, the analysis specifically focused on cells that deposited on the surface over time. In this assay, images were captured every five minutes over a two hour-period to quantify the cells depositing on the surface over time. To quantify the number of cells adhering to the surface, the images were processed using ImageJ (release 1.46, imagej.nih.gov).[42] It should be mentioned that the initial image was used as a baseline to account for the cell deposited background, and subsequent cell counts represented the increase in deposited cells over time. [43] For each coating, the experiment was performed in triplicate, and the accumulated cell numbers, along with their standard deviations, were reported.

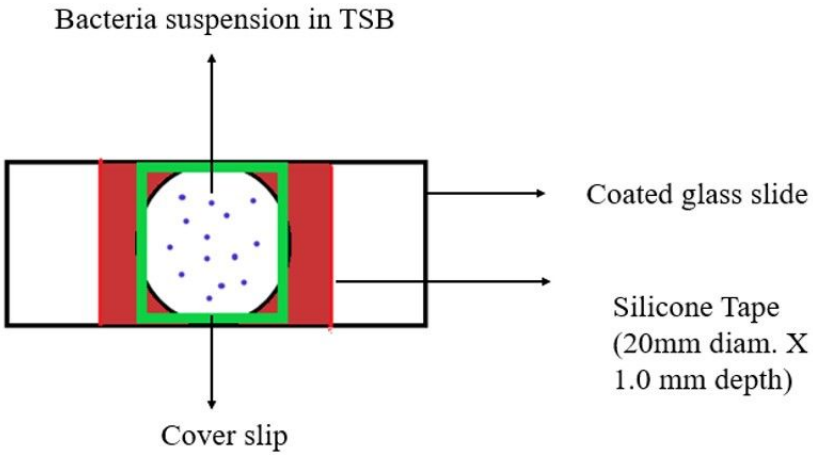

Figure 1. Illustration of the procedure employed to prepare the samples for the real-time observation of cell deposition.

2.6 Biofilm quantification experiments

For the biofilm experiments, glass slides were initially cut into 2 cm × 2 cm squares using a diamond pen and subsequently coated with ZAC polymers. These coated and non-coated substrates were then arranged in 6-well plates to assess the potential formation of biofilms by *E. coli* and *B. subtilis* on their surfaces. To prepare the cells for the experiments, *E. coli* and *B. subtilis* were grown in TSB until the late log phase (OD_{600}=0.6). Then, 1 mL of *E. coli* and *B. subtilis* cell suspensions were individually added to 5 mL of TSB solution in the 6-well plates containing the glass slides. The *E. coli* and *B. subtilis* cells were grown for 24, 48, and 72 h in the wells. Bare and ZAC-coated glass slides were taken out of the 6-well plates and dried gently with Kimwipes by allowing the solution flow to one end of the slide in a horizontal position and rinsed with PBS buffer, followed by staining with LIVE/DEAD™ BacLight™ Bacterial Viability Kit (Thermo Fisher, Invitrogen) for microscopy imaging and quantitative assays.

The staining included two dyes: Syto 9 dye (component A - green) detecting live cells at an emission range of 485-498 nm and Propidium iodide (component B – Texas red) detecting dead

cells at an emission range of 535-617 nm. After initially washing the glass slides with PBS, 3μL of each of the dyes was added to 1mL of Hank's Balanced Salt Solution (HBSS) in a separate amber tube and mixed thoroughly before adding to the glass slide. From the tube, 30μL of the solution was added to the glass slide and incubated at room temperature in the dark for 30 min. Then, the glass slides were gently dipped and washed with 1× HBSS and proceeded for imaging. The images of the biofilms on the slides were obtained by confocal laser scanning microscopy (CLSM) using the Leica DM 2500 Microscope. Measurements were determined under a 10× objective at 0.30 numerical aperture. Five image stacks, each containing five optically sectioned images (512- by 512-pixel tagged image file format) per strain were collected at random. Z-stacks were taken at 1 μm increments from the surface (the first plane in which bacteria were identified), and hence the distance from the surface was equivalent to the biofilm thickness. COMSTAT (www.imageanalysis.dk) software was used to analyze the acquired Z-stack images to determine the biomass and average thickness calculations of the biofilms (Heydorn et al. 2000). Similarly, triplicate analysis was done for each sample at each time period investigated.

3. Results and discussion

3.1 Characterization of ZAC coatings before and after conditioning with organic molecules

We studied the biofouling behavior of four different ZACs, each combining one of two hydrophobic monomers (TFEMA, termed PT; or MMA, termed PM) with one of two zwitterionic monomers (SBMA; or MPC) (**Figure 2**). According to the ^{1}H-NMR characterization reported in our previous publication, which studied the scaling behavior of the same set of ZACs, all four ZACs exhibited similar hydrophobic-to-zwitterionic monomer ratios by mass, with zwitterionic monomer contents ranging from 34 wt% to 40 wt%. [34] This ratio has been previously demonstrated

to be effective in forming membrane selective layers highly resistant to organic fouling by proteins, oils, and other organic matter, while maintaining insolubility in water.[25,26,29] Due to fluorination, PT is more hydrophobic than PM, but also contains more polar bonds. PT-based ZACs have been extensively used in previous work to create both highly fouling-resistant membranes[25,26,29] and hydrophobic yet fouling resistant materials. PM-based ZACs also form successful fouling-resistant membranes and surfaces,[26] and can also work as surface-segregating additives for fouling-resistant membranes[28]. In a study of PT-based ZAC membranes, SBMA and MPC both created highly fouling-resistant surfaces, though MPC-based copolymers exhibited higher hydrophilicity[28]. However, SBMA- and MPC-based surfaces also show differing scaling propensity,[34] which implies different surface-particle interactions. As such, it is valuable to study the effect of the chemical nature of each component of a ZAC on biofilm formation. XPS survey scans (**Figure S11, Table S4**) confirmed the presence of sulfonate (SBMA) and phosphate (MPC) groups on ZAC coatings surfaces, with similar S2p (1.4%) and P2p (2.0%) atomic ratios. These comparable functional group levels further suggest that differences in biofouling resistance stem from the intrinsic properties of the zwitterionic groups.

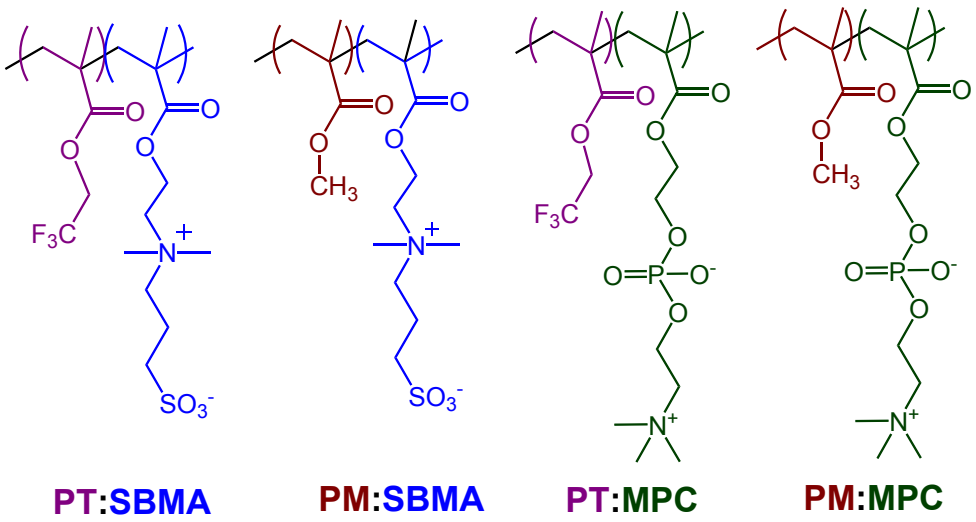

Figure 2. Chemical structures of the four ZACs used in this study

Organic matter from the growth media could interfere with the ZAC coating properties by creating a conditioning film that could facilitate cell deposition and biofilm formation. Exposure to water and salts can also cause significant morphological changes in zwitterionic amphiphilic films.[44] However, the films examined in this study remained stable when exposed to water, organic-free saline solutions, and even organic-rich media, as confirmed by AFM (**Figures S1, S2, S8**), captive air contact angle (**Figures 3, and S9**), FTIR (**Figure S10**) measurements. The effect of exposure to either an organic-free saline solution or to organic matter on the surfaces was observed by determining the changes in the captive air contact angle, surface roughness, and surface zeta potential. Before exposure to either solution, the captive air bubble contact angles (**Figure 3**) of ZAC coatings containing the MPC monomer (i.e., PT:MPC, PM:MPC) were lower than those coatings containing the SBMA monomer (i.e., PT:SBMA, PM:SBMA), which indicated that the phosphorylcholine (MPC) was more hydrophilic than the sulfobetaine (SBMA). This is in accordance with the findings in our prior study, where such a difference was attributed to lower charge density between cation and anion moieties of MPC compared to those of SBMA.[25,34]

To distinguish the impact of exposure to an aqueous salt solution on surface properties, the captive air contact angle of ZACs coatings after salt conditioning were characterized. ZAC-coated samples were immersed in an organic-free salt solution that serves as the background of the broth used in biofouling experiments (5 g/L NaCl and 2.5 g/L K_2HPO_4) for 72 hours. It was found that captive air contact angle values for PM:SBMA and PM:MPC also increased after salt conditioning compared to before conditioning. This suggests that copolymers containing MMA units may swell more readily in the presence of salt, thus affecting their surface hydrophilicity. Among these copolymers, the salt conditioning have more influence on PM:SBMA coatings than PM:MPC

coatings. This finding is consistent with our previous study, which showed that PM:SBMA is more prone to conformational changes in the presence of 100 mM NaCl solution.[25,34]

To study the effects of exposure to organic media, ZAC-coated samples were conditioned in TSB, a nutritional medium rich in organic matter (e.g. peptides, glucose) in saline used in biofouling experiments, for 72 hours. The captive air bubble contact angle values of PT:SBMA and PT:MPC showed no significant statistical difference compared to before conditioning (**Figure 3**). In contrast, captive air bubble contact angle values of PM:SBMA and PM:MPC increased by ~5^{o} after conditioning, a statistically significant change (ANOVA statistical analysis was performed comparing the ZAC polymers wherein: $p < 0.05$), indicating that their surfaces became less hydrophilic after TSB treatment. However, it is worth noting that these contact angles were similar to or lower than the contact angles obtained upon exposure to salt solutions without the organics. This implies that, while surface changes occurred, they are at least not exclusively associated with organics adsorption.

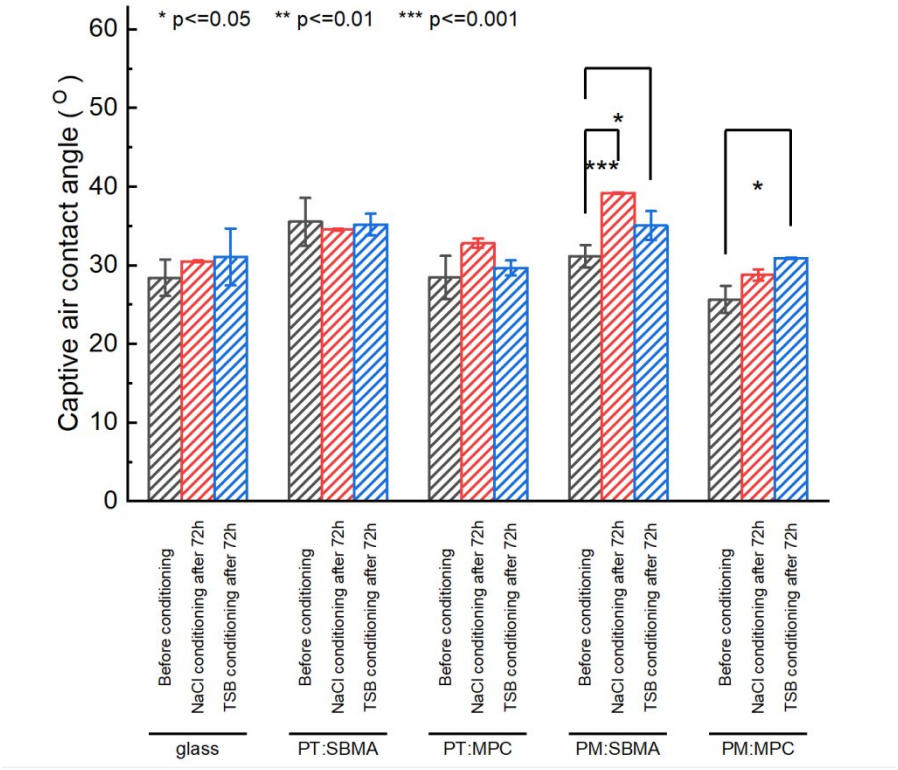

Figure 3. Captive air bubble measurement results for different ZAC coatings before and after conditioning in a mixture of 5 g/L NaCl and 2.5 g/L K_2HPO_4, and TSB media, for 72 hours. Error bars represent standard deviations of five replicates for each condition. ANOVA statistical analysis was performed to compare the ZAC polymers, where asterisks (*) indicate statistically significant differences ($p < 0.05$).

Surface hydrophilicity can be affected by surface roughness and surface charge at the molecular level. The roughness of various ZAC coatings was measured using AFM scanning and the results are presented in **Figure 4 and Figures S1-S2**. Prior conditioning, the surface roughness of PT:SBMA shows a little bit higher than those PT:MPC, whereas the surface of PM:SBMA coating was rougher than that of PM:MPC. After 72 hours of conditioning in a salt solution, the surface roughness of all copolymer coatings except PM:MPC significantly increased compared to their pre-conditioning state, while PM:MPC's surface roughness remained unchanged. These

changes indicate that the salt solution in the media tends to produce rougher surfaces except in the case of PM:MPC. This effect is likely due to the swelling and de-swelling of the copolymer coatings in the salt solution, which alters their surface morphology (**Figure S1 and 2**).[44] In contrast, after 72 hours of conditioning in the TSB solution, the surface roughness of PT:SBMA, and PM:SBMA decreases. Meanwhile, PT:MPC, and PM:MPC show an increase in surface roughness after 72 hours of TSB conditioning compared to their pre-conditioning state. The relative rougher surfaces on PM:SBMA, and PM:MPC after TSB conditioning could be responsible for the observed changes in their surface hydrophilicity. Notably, prior to conditioning, all examined ZAC coatings had a film thickness of approximately 200 nm, with no significant differences among the copolymer coatings, except for PT: SBMA, as confirmed by our prior AFM measurements.[34] Following salt and TSB conditioning, the maximum value of surface roughness can only reach 50 nm (**Figure 4**), which is still substantially smaller than the overall film thickness. This indicates that the changes in surface roughness are independent of the total film thickness and are unlikely to compromise the structural integrity or performance of the coatings.

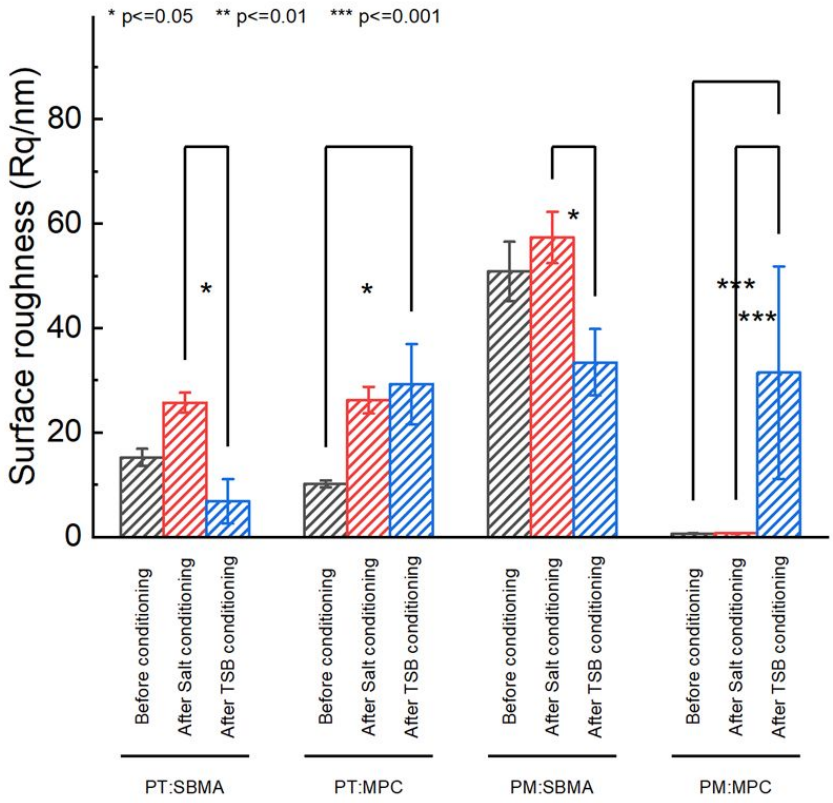

Figure 4. Surface roughness (root mean square, *Rq*) of different ZAC coatings after conditioning in TSB medium and a mixture of 5 g/L NaCl and 2.5 g/L K_2HPO_4 salt solutions for 72 hours. Representative AFM images are provided in the Supporting Information (Figures S1 and S2). Error bars represent standard deviations from measurements at three different locations per coating, both before and after conditioning. Statistically significant differences between ZAC polymers, determined by ANOVA, are indicated by asterisks ($p < 0.05$).

Besides the surface roughness, the surface zeta potential of PT:MPC, PM:SBMA, and PM:MPC measured in the TSB medium was also investigated (**Figure 5)**. To better analyze the effect of organic matter from the TSB medium on the surface charge of the ZAC coatings, the zeta potential values of ZAC coatings measured in 10mM NaCl solution from our previous publications were used as a comparison.[34] The surface zeta potential measurements in various solution environments consistently show negative values. These polymers are chemically neutral because they lack weak acidic or basic groups in their structures. However, various zwitterionic groups, especially sulfobetaines, have been shown to exhibit negative zeta potentials over a broad pH range.

This is believed to arise from the adsorption of salt ions due to interactions with zwitterionic groups, with stronger zwitterion-anion interactions resulting in an apparent net charge.[45,46] All four ZAC coatings exhibited similar zeta potentials, within error margin of each other. The surface zeta potential values for the ZAC coatings did not display any significant statistical difference upon immersion in TSB, which implied that organic media does not measurably change surface charge.

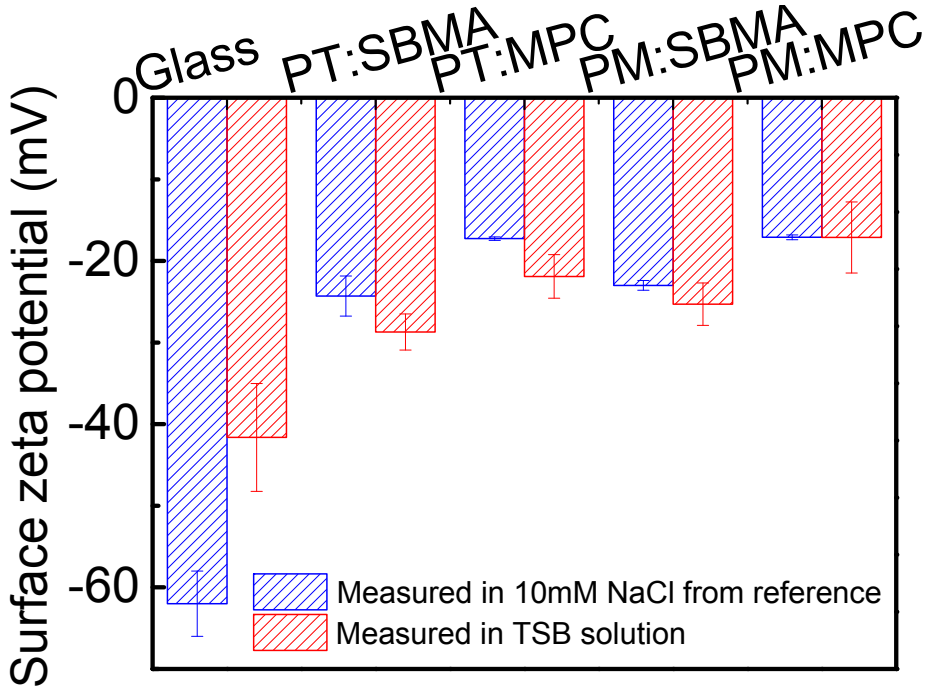

Figure 5. Surface zeta potential measurement results of different ZAC coatings measured in the TSB media and 10 mM NaCl (from our previous publication[34]). The error bars correspond to standard deviations of different time runs for each ZAC coating. Due to the limitations of the instrument's operational range for measuring surface zeta potential, a 100-fold dilution of the initially prepared TSB solution was employed to assess surface zeta potential. All these measurements were performed at room temperature. The error bars represent the standard deviation of three replicates.

To examine interactions between ZAC coatings and organic matters from TSB, ATR-FTIR spectra were collected for all ZAC coatings before and after conditioning at different time periods.

As shown in **Figure S3**, prior to conditioning, peaks were observed at 1036 and 1201 cm^{-1}, corresponding to the sulfobetaine moieties in PT:SBMA (**Figure S3A**) and PM:SBMA (**Figure S3B**), respectively. Similarly, peaks at 1086 and 1235 cm^{-1} were noted for the phosphonate moieties in PT:MPC (**Figure S3A**) and PM:MPC (**Figure S3B**), respectively, confirming successful ZAC coating. After 72 hours of TSB conditioning, it was observed a peak at ~1640 cm^{-1}, typically associated with water. This is consistent with water absorption into the ZAC materials. No other clear new peaks that would document significant adsorption of organic molecules in TSB were observed (**Figure S3**). However, prior AFM and contact angle measurements have shown that TSB conditioning does affect the surface morphology and hydrophilicity, especially for PM:SBMA and PM:MPC coatings. If any organic adsorption is occurring, it is probably below the detection threshold of the instrument.

3.2 Characterizations of bacterial surface properties

To understand the interactions between different bacterial cells and ZAC-coated substrates, *E. coli* and *B. subtilis* grown on TSB medium were investigated. As shown in **Figure 6A**, the affinity of different bacterial strains towards hexane and decane was compared. The results showed that *E. coli* exhibited similar affinity (85%) toward hexane and decane, while *B. subtilis* exhibited less affinity (70%) toward decane compared to hexane, which suggests that *B. subtilis* cell surface is less favorable for interacting with decane molecules compared to hexane. Several studies previously found that bacteria tend to differ from each other based on their hydrophilicity and surface charge properties under different solution chemistries.[47,48] The interactions between *B. subtilis* and decane were found to be smaller, suggesting a lower affinity towards non-polar solvents compared to *E. coli*. Thus, as a Gram-positive bacterium, *B. subtilis* demonstrated less hydrophobicity in comparison to *E. coli.* The results of this study align with those of a previous

investigation into the hydrophobicity profile of *E. coli K12* strains, and *B. subtilis* as shown in **Table S3**.[39] Moreover, Gram-negative *E. coli* is typically less vulnerable to organic solvents compared to Gram-positive *B. subtilis* due to their robust outer membrane, which serves as a formidable permeability barrier. In Gram-negative bacteria like *E. coli*, the presence of an outer membrane notably enhances the hydrophobicity of the cell surface.[49–51]

The average zeta potential of *E. coli*, a Gram-negative bacterium, was -14 mV in TSB medium and -20 mV in PBS. Conversely, the Gram-positive bacteria, *B. subtilis,* exhibited lower zeta-potential values. The results showed that *B. subtilis* had a zeta potential of -5 mV in TSB and -10 mV in PBS, as depicted in **Figure 6B**. The dissimilarity in surface charge between Gram-negative and Gram-positive bacteria can be attributed to the presence of an extra layer of negatively charged lipopolysaccharide in Gram-negative bacteria, which aligns with the findings of M. Arakha et al.[52] Their study also demonstrated that the surface charge of bacteria can be influenced by the presence of organic molecules in the growth media. The presence of organic molecules in TSB reduced the negativity of the zeta potential results.

(A)

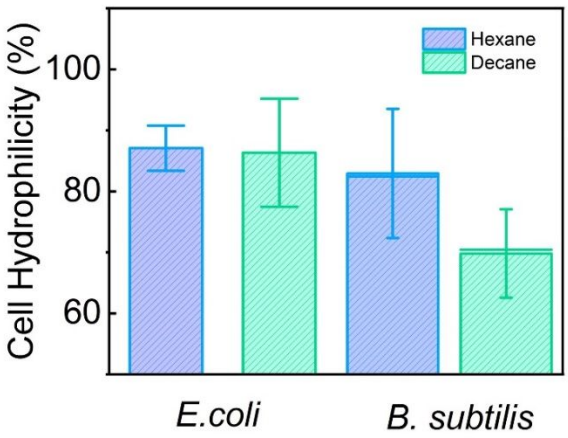

(B)

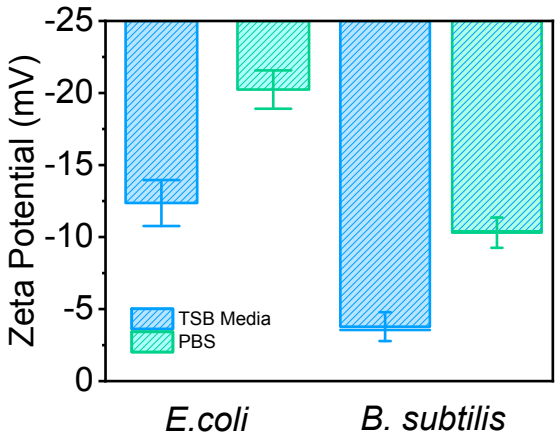

Figure 6. (A) Percentage of cell hydrophilicity of *E. coli* and *B. subtilis* in hexane and decane, ANOVA statistical analysis was performed wherein: F value: 115.02, p-value: 4.50×10^{-79} (B) Zeta potential measurements of different bacteria measured in the TSB medium and PBS. ANOVA statistical analysis was performed wherein: F value: 402.86, p-value: 1.52×10^{-38}. The error bars correspond to standard deviations from *E.coli* and *B. subtilis* samples. Both of the results were statistically significant at 0.05 level.

3.3 The roles of surface properties of ZAC coatings in controlling cell deposition/attachment

Biofouling occurs as a series of interconnected events, starting with the deposition and attachment of cells, followed by their subsequent growth and proliferation, ultimately resulting in the formation of a biofilm. Therefore, to understand the cell adhesion/attachment behavior concerning different types of ZAC coatings, the cell deposition rate of *B. subtilis* and *E. coli* onto bare and ZAC-coated glass slides were quantified as shown in **Figure 6A-B**, and **Figure S4,** respectively. By continuously monitoring the entire cell deposition process at 5-minute intervals over a span of 2 h, it was observed that the number of *B. subtilis* cells deposited on ZAC coatings (except for PT:MPC) initially increased but eventually reached a plateau after 100 min (**Figure 7A**). In contrast, the number of *E. coli* cells exhibited a consistent upward trend on all ZAC coatings throughout the same time period (**Figure 7B**). Interestingly, *B. subtilis* cell deposition on ZAC-coated surfaces was found to be lower than *E. coli* cell deposition after the whole cell deposition experiment (**Figure 7C**). Additionally, among all ZAC coatings, PT:SBMA exhibited the lowest number of *B. subtilis* and *E. coli* cell depositions (**Figures 7 , and S4**), implying that PT:SBMA surfaces have the highest potential for resisting cell attachment.

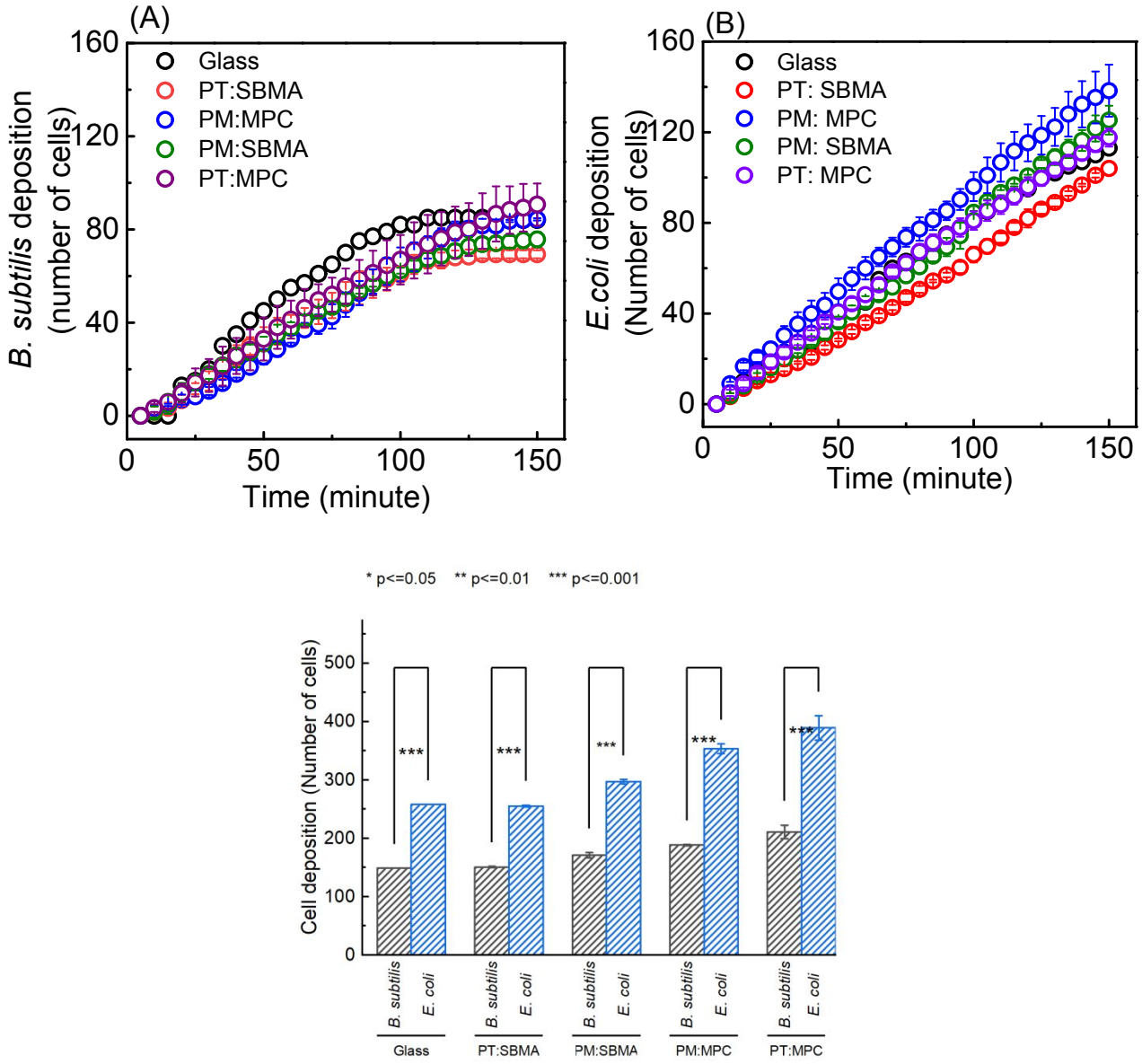

Figure 7. Quantification of cell deposition behavior of (A) *B. subtilis*, and (B) *E. coli* on different ZAC-coated surfaces throughout 2 h. (C) ANOVA analysis of cell deposition of *B. subtilis*, and *E. coli* across different substrates at the end of cell deposition process (150 min), where * represents statistically significant ($p<0.001$). Both cells were grown in TSB media and washed with PBS buffer. It should be noted that the accumulation of cells deposited was based on additional cells attaching to the surface by subtracting the background of cells on the first image. The images of the sequential cell deposition are presented in the supporting information (**Figure S4**). The error bars correspond to the standard deviations of three replicates for each type of ZAC coating. All cell deposition experiments were performed at room temperature and in PBS

To uncover the underlying mechanisms governing cell attachment on ZAC coatings, we examined the surface hydrophobicity of both cells and materials, along with their associated surface tension parameters. As previously mentioned, both *E. coli* and *B. subtilis* strains exhibited distinct hydrophobicity characteristics, with *B. subtilis* displaying lower hydrophobicity than *E. coli*. It should be mentioned that all ZAC coatings exhibited water contact angles greater than 90 degrees in the dried state, indicating their hydrophobic nature in our previous publication.[34] Therefore, it can be inferred that the initial attachment rate of *B. subtilis*, being less hydrophobic, should be smaller compared to *E. coli* on the hydrophobic surfaces.

In **Figure 3**, all ZAC coatings presented relatively low captive air contact angles when they were measured under hydration. This is because, in aqueous environment, the polymer surface undergoes local rearrangement of side groups to expose hydrophilic groups, thus creating hydrophilic surfaces.[53] However, it was found that after the conditioning with organic molecules from the growth medium, there was a reduction in the surface hydrophilicity for PM:SBMA and PM:MPC, however, this change did not occur with the PT:SBMA and PT:MPC coated surfaces. The organic molecule conditioning of the surface was responsible for enhancing the cell attachment on PM:SBMA and PM:MPC coating surfaces (**Figure 6A-B**).

In addition, it has been reported that the lower surface energy typically correlates with increased hydrophobicity, which is known to reduce fouling. According our prior finding, the surface energy of PT:SBMA and PT:MPC was lower than those of PM:SBMA and PM:MPC, PT:SBMA with the lowest surface energy among all four coatings (**Table S2**). The lower surface energy and increased hydrophobicity of PT:SBMA and PT:MPC coatings may explain their higher resistance to organic fouling and subsequent cell attachment.[34] However, it is important to note that surface energy was determined from contact angle measurements taken in air, not in

environments such as TSB media or water, where surface energy is likely higher. Additionally, hydrophobicity alone is a poor predictor of protein and heterogeneous macromolecular adsorption on chemically heterogeneous surfaces. Research suggests that adsorption is primarily influenced by the local interaction energy between foulants and surface domains and is inhibited when the length scale of foulant anchoring sites exceeds that of the surface domains.[30] Therefore, further investigation is still needed to fully understand these mechanisms in the future.

Derjaguin, Landau, Vervey, and Overbeek (DLVO) model was also used to predict the mutual interactions among ZAC coatings, microbes, and growth medium. DLVO is a basic model for characterizing the initial adherence of bacteria to particles in suspension,[48] and it has been modified for cell adhesion prediction with the extended DLVO theory (x-DLVO), which considers the interaction of repulsion caused by electrostatic charges and the attraction of Van der Waals forces between colloidal particles.[54] More details relevant to the model can be found in previous publications.[55] By referencing previously reported surface tension components of both microorganisms and TSB growth medium (**Table S1-S2**),[56,57,58] the total interfacial energy among the microbes, TSB media, and ZAC coatings was calculated as shown in **Figure 8A-B**.

As depicted In **Figure 8A**, the total free energy of interaction ($\mathbf{\Delta G_{mlc}^{T}}$) between *B. subtilis* and various coatings (i.e., PT:SBMA, PT:MPC, PM:SBMA, and PM:MPC) tended towards neutral or positive values. This indicates an unfavorable adsorption of *B. subtilis* onto ZAC coatings. It's widely recognized that the more negative the total interaction energy, the more favorable the cell adhesion.[59–62] The total interaction energies for *B. subtilis*-ZAC coatings (**Figure 8A**) were higher (less negative) compared to those of *B. subtilis*-Glass (-11.9 mJ/m^2). This elucidates why fewer *B. subtilis* cells were adsorbed onto ZAC coatings compared to glass surfaces, as illustrated in **Figure 7A**. In contrast, the total interaction energies for all four ZAC coatings with *E. coli* were negative,

suggesting attraction between *E. coli* and ZAC coatings (**Figure 8B**). Furthermore, these total interaction energies for *E. coli* were notably more negative than those for *B. subtilis*. This discrepancy can elucidate why the deposition number of *E. coli* cells was significantly higher than that of *B. subtilis* (**Figure 7C**).

It's worth noting that for both types of cells, the total interaction energy for PT:MPC was higher (less negative) compared to that of PT:SBMA. This suggests that fewer cells would be expected to deposit on PT:MPC coatings than on PT:SBMA. Interestingly, it was observed that PT:SBMA exhibited the lowest number of *B. subtilis* and *E. coli* cell depositions. Such observed fouling behaviors with the ZAC coatings were inconsistent with the x-DLVO prediction values. Hence, it seems that the total interaction energy calculated solely based on x-DLVO theory might not adequately explain the true cell adhesion phenomenon. Based on our previous study, this could be attributed to significant variations on surface chemistry (such as charge density) or morphology (such as roughness).[34] These factors can influence surface energy distribution and subsequently cell adhesion.

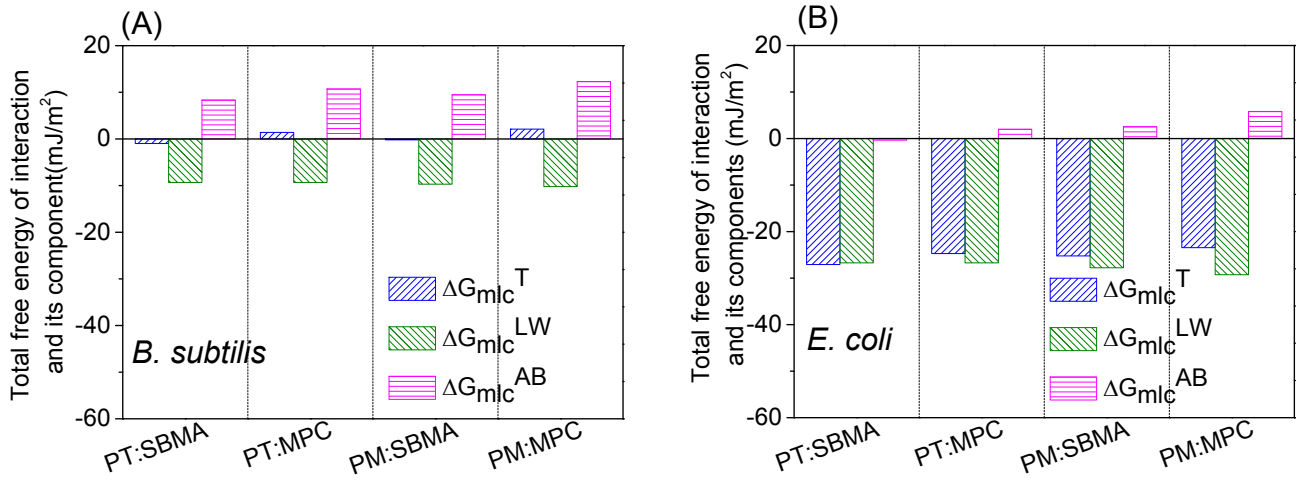

Figure 8. Total free energy of interaction (ΔG_{mlc}^{T}) and its components (Van der Waals interaction-ΔG_{mlc}^{Lw} , Lewis acid base -ΔG_{mlc}^{AB}) among the bacteria, coatings, and TSB media which were

calculated based on the DLVO prediction model for (A) *B. subtilis*, and (B) *E. coli.* From thermodynamic prediction point of view, the adhesion of bacterial cells is favorable only when the total energy of interaction is negative. The interaction energy values are applicable at the closest proximity of approximation (0.157 nm), which can be interpreted as the distance between the outer electron shells (van der Waals boundaries) of adjacent non-covalently interacting molecules.

Surface roughness plays a significant role in providing favorable sites for colonization, as rough surfaces have larger surface areas and depressions that facilitate attachment.[63,64] The changes observed in the surface roughness of ZAC coatings after conditioning with organic molecules indicate that the organic matter from the media solution tends to cause rougher surfaces on the coatings, except for PT:SBMA (**Figure 4**), thus, in turn, facilitating the cell attachment on the surface. Notably, due to *B. subtilis* having a lower surface charge (approaching neutral, **Figure 6B**), the surface charge presented a greater impact on *B. subtilis* compared to *E. coli*. Consequently, it may have restricted cell transport and even hindered the growth of biofilms in the case of *B. subtilis*.

3.4. Effects of organic conditioning ZAC coatings on the formation of biofilm

In addition to the cell deposition experiment, the biofilm layer resulting from the attachment, growth, and proliferation of *E. coli* and *B. subtilis* cells on various types of ZAC coatings was analyzed using CLSM. The biofilms were characterized by quantifying the total biomass deposition, biofilm thickness, roughness coefficient, and percentage cell death after 72 hours, as depicted in **Figure 9, and Figure S5**. The combined biomass **(Figure 9A**), and biofilm thickness (**Figure S5A**) of *B. subtilis* on all ZAC-coated surfaces were observed to be lower than those on uncoated glass slides. Conversely, the total biomass (**Figure 9B**) and biofilm thickness (**Figure S5B**) of *E. coli* did not show any statistically significant differences between bare glass surfaces and four ZAC-coated surfaces. Notably, *B. subtilis* biofilm resulted in reduced biomass and biofilm

thickness on all four ZAC-coated surfaces compared to *E. coli;* though there was no significant difference among different ZAC coatings. The biofilm quantification results further confirmed that ZAC coatings showed better resistance to the biofilm formation caused by *B. subtilis* than by *E. coli*. This is consistent with the previous quantification results of cell attachment where ZAC coatings were less favorable for the cell attachment of *B. subtilis* than *E. coli*. Similar findings were observed when analyzing the percentage of cell death. The percentage of cell death for *B. subtilis* (**Figure 9C**) showed no significant differences between bare glass slides and the four ZAC-coated surfaces. However, for *E. coli* (**Figure 9D**), the percentage of cell death on bare glass slides was lower compared to the ZAC-coated surfaces. This suggests that the chemistry of the ZAC-coated surfaces enhances detachment-induced cell death in *E. coli* more effectively than in *B. subtilis*. This difference is likely attributable to variations in the cell membrane structure between the two bacterial species.[65–67] Further investigation into this phenomenon is warranted but falls outside the scope of the current study.

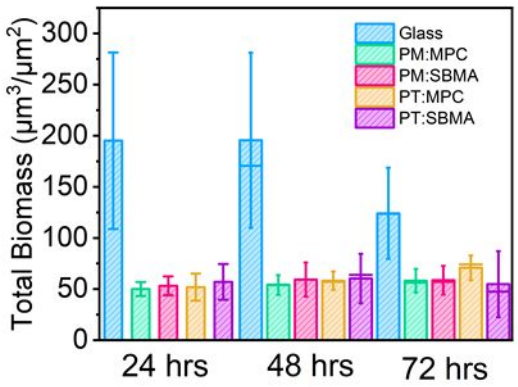

(A)

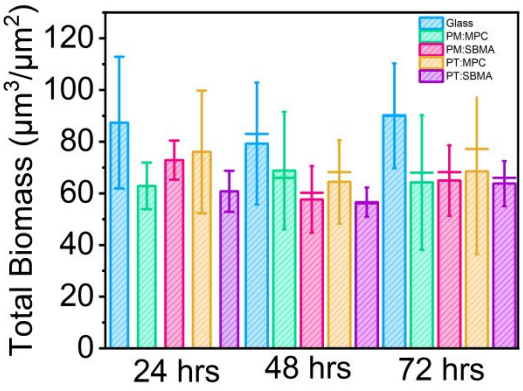

(B)

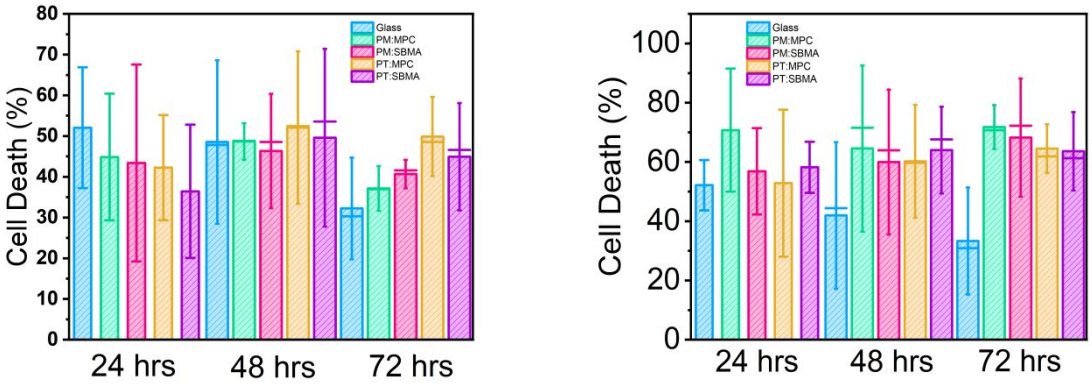

Figure 9. CLSM results related to total biomass and average thickness for bare and ZAC-coated glass for *B. subtilis* (A, and C), and E. *coli* (B, and D) at room temperature. The standard deviations are represented in the graph as error bars.

To establish a stronger connection between biofilm formation and cell attachment on various ZAC coatings, the bacterial deposition kinetics of both *B. subtilis* and *E.coli* were quantified by calculating the bacterial transfer rate coefficient.[39] More calculation details can be found in the supporting information (**Text S2**). As shown in **Figure S6,** the cell deposition kinetics of both microorganisms on various ZAC coatings exhibited a similar pattern, with the only distinction being the lower initial attachment rate for *B. subtilis* (**Figure S6A**) compared to *E. coli* (**Figure S6B**). However, with time, both microorganisms reached a saturated phase in which the number of attached cells became stabilized, and no further attachment occurred. These model calculations have two significant implications: Firstly, the calculated difference in the initial attachment rate aligns with the experimental findings in the cell deposition experiments. Secondly, the limited kinetics of cell attachment over time ultimately hinder the formation of biofilm on all ZAC coating surfaces, resulting in negligible differences in biofilm quantification among the different ZAC coatings. Nevertheless, when compared to glass slides, it was evident that ZACs exhibited superior effectiveness in inhibiting attachment of *B. subtilis* cells, and thereby enhancing resistance against

biofilm formation. In contrast, all ZAC coatings, except PT: SBMA, facilitated the deposition of *E. coli* cells, promoting biofilm formation. Among the ZAC coatings tested, PT: SBMA coating displayed the highest potential for resisting biomolecule conditioning, leading to unfavorable cell attachment and further biofilm formation.

5. Conclusions

In this study, zwitterionic amphiphilic copolymers were synthesized using different zwitterion monomers (i.e. SBMA, and MPC) and hydrophobic monomers (i.e. TFEMA, and MMA). Exposure of ZAC coatings to the growth media led to changes in surface roughness and contact angle, which influenced cell attachment and biofilm formation. Bacterial cell deposition (i.e., *B. subtilis*, and *E. coli*), and biofouling experiments on various ZAC coatings revealed that both types of bacteria showed a tendency to deposit on the coatings. However, it was observed that all ZAC coatings exhibited higher resistance to the attachment of *B. subtilis* compared to *E. coli*, which consequently hindered the formation of biofilms on the coated surfaces. This can be attributed to the decreased hydrophilicity of *B. subtilis*. Conditioning with PM:SBMA and PM:MPC resulted in reduced hydrophilicity, making it easier for bacteria to adhere. Among the tested ZAC coatings, PT:SBMA demonstrated the highest potential for resisting cell attachment, likely due to its lower surface roughness after conditioning with TSB. In summary, the deposition rate of cells varied depending on the type of bacteria and the type of ZAC coating. Therefore, to design anti-biofouling coatings, the selection of ZAC coatings should consider the type of bacterial strains and their anti-fouling mechanisms.

Supporting information

The Supporting Information includes the materials, ZAC synthesis protocols, Definition of the bacterial deposition kinetics, Derjagiun-Landau-Verwey-Overbeek (DLVO) model, and biofilm quantification results.

Author information

Corresponding Authors

*Debora F. Rodrigues− Department of Environmental Engineering and Earth Sciences, Clemson University, Clemson, South Carolina, 29634, United States; orcid.org/0000-0002-3124-1443; Phone: 864-656-3519; Email: dfrodri@clemson.edu.

Authors

Meng Wang−Department of Civil & Environmental, Engineering, University of Houston, Houston, Texas 77004, United States;

Murchana Sarma – Department of Materials Science and Engineering, University of Houston, Houston, Texas 77004, United States, Department of Environmental Engineering and Earth Sciences, Clemson University, Clemson, South Carolina, 29634, United States

Samuel J. Lounder − Department of Chemical and Biological Engineering, Tufts University, Medford, Massachusetts 02155, United States;

Abhishek N. Mondal − Department of Chemical and Biological Engineering, Tufts University, Medford, Massachusetts 02155, United States;

Ayse Asatekin − Department of Chemical and Biological Engineering, Tufts University, Medford,

Massachusetts 02155, United States;

Lavanya Muthusamy − Holcombe Department of Electrical and Computer Engineering, Clemson University, Clemson, South Carolina 29634, United States

Goutam Koley − Holcombe Department of Electrical and Computer Engineering, Clemson University, Clemson, South Carolina 29634, United States

Notes

The authors declare no competing financial interest

Acknowledgment

This study is based upon work supported by the National Science Foundation under Grant Nos. CHE-1904472 and CHE-1904465.

REFERENCES

(1) Filloux, E.; Wang, J.; Pidou, M.; Gernjak, W.; Yuan, Z. Biofouling and Scaling Control of Reverse Osmosis Membrane Using One-Step Cleaning-Potential of Acidified Nitrite Solution as an Agent. *J. Memb. Sci.* **2015**, *495*, 276–283.

(2) Yang, S.; Song, Z.; Li, P.; Sun, F.; Zeng, H.; Dong, W. Biofouling Initiation on a Microfiltration Membrane Related to Deposition and Adhesion of Bacteria from the Perspective of Interface Interactions. *Desalination* **2023**, *545, 116151*.

(3) Farkas, A.; Degiuli, N.; Martić, I. The Impact of Biofouling on the Propeller Performance. *Ocean Eng.* **2021**, *219*, 108376.

(4) Matin, A.; Khan, Z.; Zaidi, S. M. J.; Boyce, M. C. Biofouling in Reverse Osmosis Membranes for Seawater Desalination: Phenomena and Prevention. *Desalination* **2011**, *281* (1), 1–16.

(5) Harding, J. L.; Reynolds, M. M. Combating Medical Device Fouling. *Trends in Biotechnology*. **2014**, 140–146.

(6) Koschitzki, F.; Wanka, R.; Sobota, L.; Gardner, H.; Hunsucker, K. Z.; Swain, G. W.; Rosenhahn, A. Amphiphilic Zwitterionic Acrylate/Methacrylate Copolymers for Marine Fouling-Release Coatings. *Langmuir* **2021,** 37, 5591−5600.

(7) Arabaghian, H.; Wang, M.; Ordonez, J.; Rodrigues, D. F. Chapter 2 - Zwitterionic Polymers in Biofouling and Inorganic Fouling Mechanisms; Tseng, H.-H., Lau, W. J., Al-Ghouti, M. A., An, L. B. T.-60 Y. of the L.-S. M., Eds.; Elsevier, **2022**; 33–70.

(8) Shafi, H. Z.; Matin, A.; Khan, Z.; Khalil, A.; Gleason, K. K. Surface Modification of Reverse Osmosis Membranes with Zwitterionic Coatings: A Potential Strategy for Control of Biofouling. *Surf. Coatings Technol.* **2015**, *279*, 171–179.
(9) Marré Tirado, M. L.; Bass, M.; Piatkovsky, M.; Ulbricht, M.; Herzberg, M.; Freger, V. Assessing Biofouling Resistance of a Polyamide Reverse Osmosis Membrane Surface-Modified with a Zwitterionic Polymer. *J. Memb. Sci.* **2016**, *520*, 490–498.
(10) Wang, Z.; van Andel, E.; Pujari, S. P.; Feng, H.; Dijksman, J. A.; Smulders, M. M. J.; Zuilhof, H. Water-Repairable Zwitterionic Polymer Coatings for Anti-Biofouling Surfaces. *J. Mater. Chem. B* **2017**, *5*, 6728.
(11) Erathodiyil, N.; Chan, H. M.; Wu, H.; Ying, J. Y. Zwitterionic Polymers and Hydrogels for Antibiofouling Applications in Implantable Devices. *Materials Today*. **2020**, 84–98.
(12) Guo, Y.; Liu, C.; Liu, H.; Zhang, J.; Li, H.; Zhang, C. Contemporary Antibiofouling Modifications of Reverse Osmosis Membranes: State-of-the-Art Insights on Mechanisms and Strategies. *Chem. Eng. J.* **2022**, *429*, 132400.
(13) Yang, S.; Song, Z.; Li, P.; Sun, F.; Zeng, H.; Dong, W.; Feng, X.; Ren, N. Biofouling Initiation on a Microfiltration Membrane Related to Deposition and Adhesion of Bacteria from the Perspective of Interface Interactions. *Desalination* **2023**, *545*, 116151.
(14) Yang, J.-C.; Zhao, C.; Hsieh, I.-F.; Subramanian, S.; Liu, L.; Cheng, G.; Li, L.; Cheng, S.; Zheng, J. Strong Resistance of Poly (Ethylene Glycol) Based L-tyrosine Polyurethanes to Protein Adsorption and Cell Adhesion. *Polym. Int.* **2012**, *61*, 616–621.
(15) Chen, S.; Li, L.; Zhao, C.; Zheng, J. Surface Hydration: Principles and Applications toward Low-Fouling/Nonfouling Biomaterials. *Polymer (Guildf).* **2010**, *51* (23), 5283–5293.
(16) Wu, J.; Chen, S. Investigation of the Hydration of Nonfouling Material Poly(Ethylene Glycol) by Low-Field Nuclear Magnetic Resonance. *Langmuir* **2012**, *28* (4), 2137–2144.
(17) Zhao, C.; Zhao, J.; Li, X.; Wu, J.; Chen, S.; Chen, Q.; Wang, Q.; Gong, X.; Li, L.; Zheng, J. Probing Structure-Antifouling Activity Relationships of Polyacrylamides and Polyacrylates. *Biomaterials* **2013**, *34* (20), 4714–4724.
(18) Laschewsky, A. Structures and Synthesis of Zwitterionic Polymers. *Polymers (Basel).* **2014**, *6* (5), 1544–1601.
(19) Meyer, B. Approaches to Prevention, Removal and Killing of Biofilms. *Int. Biodeterior. Biodegrad.* **2003**, *51* (4), 249–253.
(20) Zhang, M.; Yu, P.; Xie, J.; Li, J. Recent Advances of Zwitterionic-Based Topological Polymers for Biomedical Applications. *J. Mater. Chem. B* **2022**, *10* (14), 2338–2356.
(21) Poncin-Epaillard, F.; Vrlinic, T.; Debarnot, D.; Mozetic, M.; Coudreuse, A.; Legeay, G.; El Moualij, B.; Zorzi, W. Surface Treatment of Polymeric Materials Controlling the Adhesion of Biomolecules. *J. Funct. Biomater.* **2012**, *3* (3), 528–543.
(22) Li, D.; Wei, Q.; Wu, C.; Zhang, X.; Xue, Q.; Zheng, T.; Cao, M. Superhydrophilicity and Strong Salt-Affinity: Zwitterionic Polymer Grafted Surfaces with Significant Potentials Particularly in Biological Systems. *Adv. Colloid Interface Sci.* **2020**, *278*, 102141.
(23) Zhou, X.; Sun, Y.; Shen, S.; Li, Y.; Bai, R. Highly Effective Anti-Organic Fouling Performance of a Modified Pvdf Membrane Using a Triple-Component Copolymer of p(Stx-Co-Maay)-g-Fpegz as the Additive. *Membranes*. **2021**, *11*, 951
(24) Lounder, S. J.; Asatekin, A. Zwitterionic Ion-Selective Membranes with Tunable Subnanometer Pores and Excellent Fouling Resistance. *Chem. Mater.* **2021**, *33* (12), 4408–4416.
(25) Bengani-Lutz, P.; Converse, E.; Cebe, P.; Asatekin, A. Self-Assembling Zwitterionic

Copolymers as Membrane Selective Layers with Excellent Fouling Resistance: Effect of Zwitterion Chemistry. *ACS Appl. Mater. Interfaces* **2017**, *9* (24), 20859–20872.

(26) Bengani, P.; Kou, Y.; Asatekin, A. Zwitterionic Copolymer Self-Assembly for Fouling Resistant, High Flux Membranes with Size-Based Small Molecule Selectivity. *J. Memb. Sci.* **2015**, *493*, 755–765.

(27) Ozcan, S.; Kaner, P.; Thomas, D.; Cebe, P.; Asatekin, A. Hydrophobic Antifouling Electrospun Mats from Zwitterionic Amphiphilic Copolymers. *ACS Appl. Mater. Interfaces* **2018**, *10* (21), 18300–18309.

(28) Kaner, P.; Rubakh, E.; Kim, D. H.; Asatekin, A. Zwitterion-Containing Polymer Additives for Fouling Resistant Ultrafiltration Membranes. *J. Memb. Sci.* **2017**, *533*, 141–159.

(29) Bengani-Lutz, P.; Zaf, R. D.; Culfaz-Emecen, P. Z.; Asatekin, A. Extremely Fouling Resistant Zwitterionic Copolymer Membranes with ~ 1 Nm Pore Size for Treating Municipal, Oily and Textile Wastewater Streams. *J. Memb. Sci.* **2017**, *543*, 184–194.

(30) Dudchenko, A. V; Bengani-Lutz, P.; Asatekin, A.; Mauter, M. S. Foulant Adsorption to Heterogeneous Surfaces with Zwitterionic Nanoscale Domains. *ACS Appl. Polym. Mater* **2020**, *2020*, 4709–4718.

(31) Kaner, P.; Dudchenko, A. V.; Mauter, M. S.; Asatekin, A. Zwitterionic Copolymer Additive Architecture Affects Membrane Performance: Fouling Resistance and Surface Rearrangement in Saline Solutions. *J. Mater. Chem. A* **2019**, *7* (9), 4829–4846.

(32) Wang, S. Y.; Fang, L. F.; Cheng, L.; Jeon, S.; Kato, N.; Matsuyama, H. Improved Antifouling Properties of Membranes by Simple Introduction of Zwitterionic Copolymers via Electrostatic Adsorption. *J. Memb. Sci.* **2018**, *564*, 672–681.

(33) Erkoc-Ilter, S.; Saffarimiandoab, F.; Guclu, S.; Koseoglu-Imer, D. Y.; Tunaboylu, B.; Menceloglu, Y.; Koyuncu, I.; Unal, S. Surface Modification of Reverse Osmosis Desalination Membranes with Zwitterionic Silane Compounds for Enhanced Organic Fouling Resistance. *Cite This Ind. Eng. Chem. Res* **2021**, *60*, 5133–5144.

(34) Wang, M.; Nguyen, H.; Lounder, S. J.; Asatekin, A.; Rodrigues, D. F. Calcium Sulfate Formation on Different Zwitterionic Amphiphilic Copolymer Substrates for Salt Water Treatment. *ACS Appl. Polym. Mater.* **2022**, *4* (10), 7090–7101.

(35) Kaner, P.; Rubakh, E.; Kim, D. H.; Asatekin, A. Zwitterion-Containing Polymer Additives for Fouling Resistant Ultrafiltration Membranes. *J. Memb. Sci.* **2017**, *533*, 141–159.

(36) Ansari, A.; Peña-Bahamonde, J.; Wang, M.; Shaffer, D. L.; Hu, Y.; Rodrigues, D. F. Polyacrylic Acid-Brushes Tethered to Graphene Oxide Membrane Coating for Scaling and Biofouling Mitigation on Reverse Osmosis Membranes. *J. Memb. Sci.* **2021**, *630*, 119308.

(37) Wang, M.; Cao, B.; Hu, Y.; Rodrigues, D. F. Mineral Scaling on Reverse Osmosis Membranes: Role of Mass, Orientation, and Crystallinity on Permeability. *Environ. Sci. Technol.* **2021**, *55* (23), 16110–16119.

(38) Malvern Instruments. Surface Zeta Potential Cell. Malvern Instruments Ltd. **2011**, 1086581.https://www.avicenna.ac.ir/documents/research/fa/corefacility/zetasizer/man0483-1.0-surface-zeta-potential-cell-zen 1020.pdf.

(39) Rodrigues, D. F.; Elimelech, M. Role of Type 1 Fimbriae and Mannose in the Development of Escherichia Coli K12 Biofilm: From Initial Cell Adhesion to Biofilm Formation. *Biofouling* **2009**, *25* (5), 401–411.

(40) Katsutoshi, H.; Hisami, W.; Shun'ichi, I.; Yasunori, T.; Hajime, U. Monolayer Adsorption of a "Bald" Mutant of the Highly Adhesive and Hydrophobic Bacterium Acinetobacter Sp. Strain Tol 5 to a Hydrocarbon Surface. *Appl. Environ. Microbiol.* **2008**, *74* (8), 2511–2517.

(41) J., de K. A.; Menachem, E. Impact of Alginate Conditioning Film on Deposition Kinetics of Motile and Nonmotile Pseudomonas Aeruginosa Strains. *Appl. Environ. Microbiol.* **2007**, *73* (16), 5227–5234.
(42) Tinevez, J.-Y.; Perry, N.; Schindelin, J.; Hoopes, G. M.; Reynolds, G. D.; Laplantine, E.; Bednarek, S. Y.; Shorte, S. L.; Eliceiri, K. W. TrackMate: An Open and Extensible Platform for Single-Particle Tracking. *Methods* **2017**, *115*, 80–90.
(43) Giorgi, F.; Curran, J. M.; Patterson, E. A. Real-Time Monitoring of the Dynamics and Interactions of Bacteria and the Early-Stage Formation of Biofilms. *Sci. Rep.* **2022**, *12* (1), 18146.
(44) Kaner, P.; Sadeghi, I.; Asatekin, A. Porous Thin Films with Hierarchical Structures Formed by Self-Assembly of Zwitterionic Comb Copolymers. *Appl. Surf. Sci. Adv.* **2023**, *13*, 100361.
(45) Kurowska, M.; Eickenscheidt, A.; Al-Ahmad, A.; Lienkamp, K. Simultaneously Antimicrobial, Protein-Repellent, and Cell-Compatible Polyzwitterion Networks: More Insight on Bioactivity and Physical Properties. *ACS Appl. Bio Mater.* **2018**, *1* (3), 613–626.
(46) Kurowska, M.; Eickenscheidt, A.; Guevara-Solarte, D.-L.; Widyaya, V. T.; Marx, F.; Al-Ahmad, A.; Lienkamp, K. A Simultaneously Antimicrobial, Protein-Repellent, and Cell-Compatible Polyzwitterion Network. *Biomacromolecules* **2017**, *18* (4), 1373–1386.
(47) C, van L. M.; Lyklema, J.; Norde, W.; Schraa, G.; Zehnder, A. J. The Role of Bacterial Cell Wall Hydrophobicity in Adhesion. *Appl. Environ. Microbiol.* **1987**, *53* (8), 1893–1897.
(48) C, van L. M.; Lyklema, J.; Norde, W.; Zehnder, A. J. Influence of Interfaces on Microbial Activity. *Microbiol. Rev.* **1990**, *54* (1), 75–87.
(49) De-la-Pinta, I.; Cobos, M.; Ibarretxe, J.; Montoya, E.; Eraso, E.; Guraya, T.; Quindós, G. Effect of Biomaterials Hydrophobicity and Roughness on Biofilm Development. *J. Mater. Sci. Mater. Med.* **2019**, *30* (7), 77.
(50) Krasowska, A.; Sigler, K. How Microorganisms Use Hydrophobicity and What Does This Mean for Human Needs? *Front. Cell. Infect. Microbiol.* ***2014****, 4*, 1-7.
(51) Dyrda, G.; Boniewska-Bernacka, E.; Man, D.; Barchiewicz, K.; Słota, R. The Effect of Organic Solvents on Selected Microorganisms and Model Liposome Membrane. *Mol. Biol. Rep.* **2019**, *46* (3), 3225–3232.
(52) Arakha, M.; Pal, S.; Samantarrai, D.; Panigrahi, T. K.; Mallick, B. C.; Pramanik, K.; Mallick, B.; Jha, S. Antimicrobial Activity of Iron Oxide Nanoparticle upon Modulation of Nanoparticle-Bacteria Interface. *Sci. Rep.* **2015**, *5* (1), 14813.
(53) Wang, M.; Zuo, X.; Jacovone, R. M. S.; O'Hara, R.; Mondal, A. N.; Asatekin, A.; Rodrigues, D. F. Influence of Zwitterionic Amphiphilic Copolymers on Heterogeneous Gypsum Formation: A Promising Approach for Scaling Resistance. *Water Res.* **2024**, *266*, 122439.
(54) Perni, S.; Preedy, E. C.; Prokopovich, P. Success and Failure of Colloidal Approaches in Adhesion of Microorganisms to Surfaces. *Adv. Colloid Interface Sci.* **2014**, *206*, 265–274.
(55) Huang, X.; Li, C.; Zuo, K.; Li, Q. Predominant Effect of Material Surface Hydrophobicity on Gypsum Scale Formation. *Environ. Sci. Technol.* **2020**, 15395-15404.
(56) Harimawan, A.; Zhong, S.; Lim, C.-T.; Ting, Y.-P. Adhesion of B. Subtilis Spores and Vegetative Cells onto Stainless Steel – DLVO Theories and AFM Spectroscopy. *J. Colloid Interface Sci.* **2013**, *405*, 233–241.
(57) Abu-Lail, N. I.; Camesano, T. A. Specific and Nonspecific Interaction Forces Between Escherichia Coli and Silicon Nitride, Determined by Poisson Statistical Analysis. *Langmuir* **2006**, *22* (17), 7296–7301.

(58) Hiremath, N. Adsorption and Bacterial Adhesion Characteristics of Proteins, Microbial Growth Media and Milk on Abiotic Surfaces under Static and Laminar Flow Conditions, McGill University, CA, 2014.

(59) Sojoudi, H.; Nemani, S. K.; Mullin, K. M.; Wilson, M. G. A Micro / Nanoscale Approach for Studying Scale Formation and Developing Scale-Resistant Surfaces. *ACS Appl. Mater. Interfaces.* **2019** 11 (7), 7330-7337

(60) Teng, F.; Zeng, H.; Liu, Q. Understanding the Deposition and Surface Interactions of Gypsum. *J. Phys. Chem. C* **2011**, *115* (35), 17485–17494.

(61) Zhao, Q.; Liu, Y.; Wang, C.; Wang, S.; Müller-Steinhagen, H. Effect of Surface Free Energy on the Adhesion of Biofouling and Crystalline Fouling. *Chem. Eng. Sci.* **2005**, *60*, 4858–4865.

(62) Azimi, G.; Cui, Y.; Sabanska, A.; Varanasi, K. K. Scale-Resistant Surfaces: Fundamental Studies of the Effect of Surface Energy on Reducing Scale Formation. *Appl. Surf. Sci.* **2014**, *313*, 591–599.

(63) Bhattacharjee, S.; Ko, C.-H.; Elimelech, M. DLVO Interaction between Rough Surfaces. *Langmuir* **1998**, *14* (12), 3365–3375.

(64) Sharma, S.; Andrea Jaimes-Lizcano, Y.; McLay, R. B.; Cirino, P. C.; Conrad, J. C. Subnanometric Roughness Affects the Deposition and Mobile Adhesion of Escherichia Coli on Silanized Glass Surfaces. *Langmuir* **2016**, *32*, 5422–5433.

(65) Christova, N.; Tuleva, B.; Nikolova-Damyanova, B. Enhanced Hydrocarbon Biodegradation by a Newly Isolated Bacillus Subtilis Strain. **2004**, *59* (3–4), 205–208.

(66) Colilla, M.; Izquierdo-Barba, I.; Vallet-Regí, M. The Role of Zwitterionic Materials in the Fight against Proteins and Bacteria. *Medicines **2018**, 5, 125*.

(67) Chagnot, C.; Zorgani, M. A.; Astruc, T.; Desvaux, M. Proteinaceous Determinants of Surface Colonization in Bacteria: Bacterial Adhesion and Biofilm Formation from a Protein Secretion Perspective. *Front. Microbiol.* **2013**, *4*.

Graphical abstract

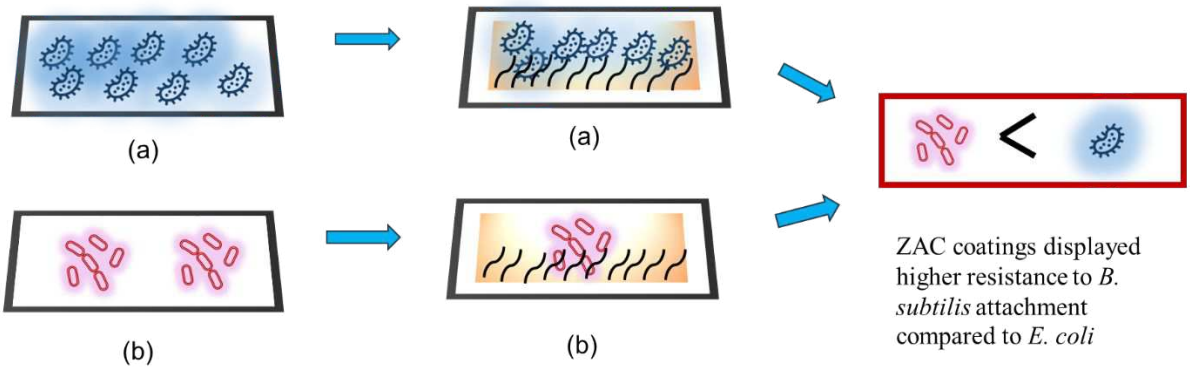

Uncoated glass substrate with (a) *E.coli* & (b) *B. subtilis*

ZAC coated glass substrate with (a) *E.coli* & (b) *B. subtilis*